Journal of Geophysical Research: Biogeosciences

Supporting Information for

Silicon Isotopes highlight the role of glaciated fjords in modifying coastal waters

J. E. Hatton,[1,2]† H. C. Ng, [2,3]† L. Meire,[4] E. M. S. Woodward, [5] M. J. Leng,[6] C. D. Coath,[2] A. Stuart-Lee,[8] T. Wang,[2] A. L. Annett,[9] and K. R. Hendry,[2,10]

[1]Department of Ecology, Charles University, Prague, Czechia

[2]School of Earth Sciences, University of Bristol. Bristol, UK

[3]Ifremer, Université Bretagne Occidentale, CNRS, Geo-Ocean, 29280, Plouzané, France

[4]Greenland Climate Research Centre (GCRC), Greenland Institute of Natural Resources, Nuuk, Greenland

[5]Plymouth Marine Laboratory, Prospect Place, The Hoe, Plymouth PL1 3DH, UK

[6]NERC Isotope Geosciences Facility, British Geological Survey, Keyworth, Nottingham NG12 3GG, UK

[7]Centre for Environmental Geochemistry, School of Biosciences, Sutton Bonington Campus, University of Nottingham, Loughborough LE12 5RD, UK

[8]Department of Estuarine and Delta Systems, Royal Netherlands Institute for Sea Research, Yerseke, The Netherlands

[9]Ocean and Earth Science, University of Southampton, Waterfront Campus, National Oceanography Centre

[10]Polar Oceans Team, British Antarctic Survey, Cambridge, UK

Contents of this file

Text S1 – Silicon Isotope Composition Analysis – Detailed Methodology

Water samples collected for dissolved silicon isotopic composition analysis ($\delta^{30}Si_{DSi}$) were filtered immediately in the field via a 0.2µm Acropak filter cartridge and kept refrigerated until analysis. However, many of these samples were problematic to analyse, especially at low DSi concentrations, with data points having high Mg corrections and/or mass dependency issues (SI Fig. 1).

We completed a series of systematic tests to better purify the samples before and after Mg-induced co-precipitation (MAGIC) and column chemistry to investigate the cause of these issues and hypothesised that the issues in analysis were likely caused due by complex organic interferences. First, we attempted to breakdown the organic matrix by exposing the samples to UV-c for up to 24 hours. However, this resulted in an unstable signal and apparent carry over of Si within the system, due to elevated blank intensities after sample introduction. Therefore, we completed further tests in an attempt to breakdown the organic material further prior to analysis, via a combination of UV-c exposure, H_2O_2 additions and oxygenation. These treatments all still resulted in partial breakdown of the organic material, leading to varying $\delta^{30}Si_{DSi}$ compositions, Mg corrections and mass dependency issues (SI Table 1).

This incomplete breakdown suggested that the organic material may be within a colloidal phase, rather than truly dissolved. There is evidence of organic colloidal phases in seawater, including humic substances and freshly produced aquagenic exopolymeric substances (EPS) i.e., from phytoplankton and bacteria. Therefore, we filtered the samples via 0.02 µm disposal syringe filters prior to MAGIC and the standard cationic column exchange purification. The additional filtration step did not impact the Si yield but significantly improved the reproducibility of $\delta^{30}Si_{DSi}$ data, reducing large Mg corrections and removing the mass dependency issues (SI Table 1, SI Fig. 1). Any samples with Mg corrections above 0.25 ‰ were discarded and reanalysed, as this suggested potential matrix issues still hadn't been resolved. We chose to filter prior to MAGIC to remove the potential for co-precipitation of Si phases with organic matrix, which would then be removed during later filtration.

Text S2 – ASi dissolution for isotope mass balance

We can calculate the amount of glacial ASi that is required to undergo dissolution to explain the discrepancies between the modelled $\delta^{30}Si_{DSi}$ composition and observed $\delta^{30}Si_{DSi}$ values from each surface sample in Nuup Kangerlua (NK) using SI equation 1:

SI Equation 1: $ASi\ required = \frac{(Observed\ \delta^{30}Si_{DSi} - Modelled\ \delta^{30}Si_{DSi})}{Glacial\ \delta^{30}Si_{ASi}}$

Where; Glacial $\delta^{30}Si_{ASi}$ composition = -0.39 ‰ and [ASi] = 58μM (based on the average values from the glacial compilation from Hatton et al. 2019).

This was completed for the closed and open model scenarios, with starting conditions of a mixed water mass (i.e., equivalent to 15 PSU). This was a mix of glacial meltwater, taken as an average from the glacial compilation of DSi and $\delta^{30}Si_{DSi}$ composition from Hatton et al. (2019) and an average of DSi concentration and $\delta^{30}Si_{DSi}$ composition from the Fram Strait, as the seawater endmember. Table S5 shows the concentrations of glacial ASi required to undergo dissolution for close the mass balance between the modelled and observed values, for each value of ε. We also report what percentage this equates to, when compared to the average ASi concentration measured for a range of glacial catchments (57.96 μM, Hatton et al., 2019).

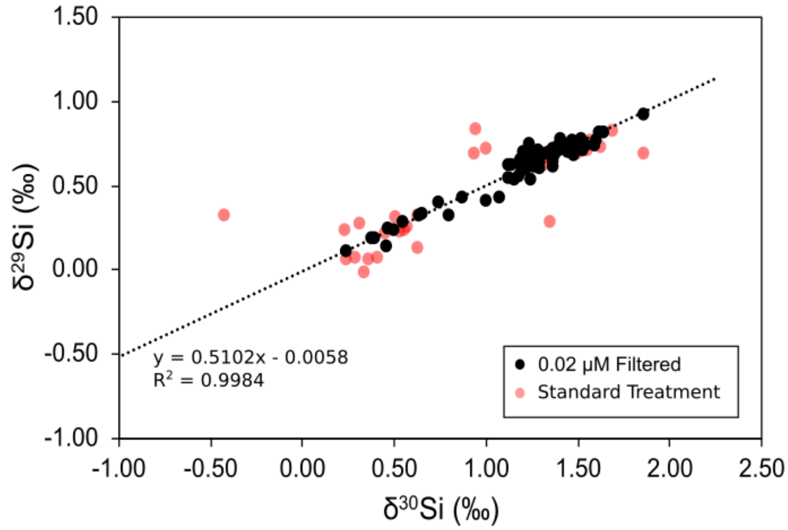

Figure S1. Three isotope plot highlighted the difference in data quality when using standard chemical preparation (red) and after additional filtration (black). Black dotted trend line is the linear regression for the 0.02 µM filtered (black) samples only.

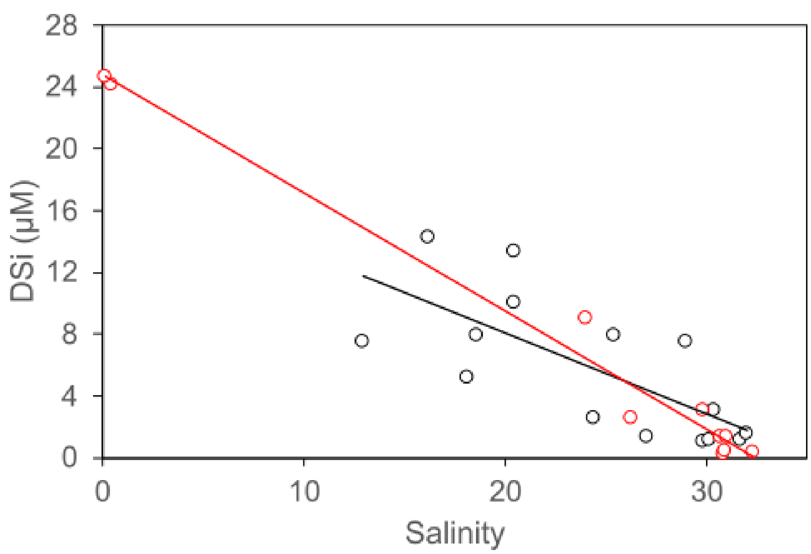

Figure S2. Scatter plot of dissolved silicon concentration (DSi) and salinity for surface samples (< 5 m depth) for Nuup Kangerlua (NK, black) and Ameralik Fjord (AM, red). Linear regressions are statisitically significant (NK; $p = 3.4 \times 10^{-6}$, AM: $p = 1.1 \times 10^{-12}$).

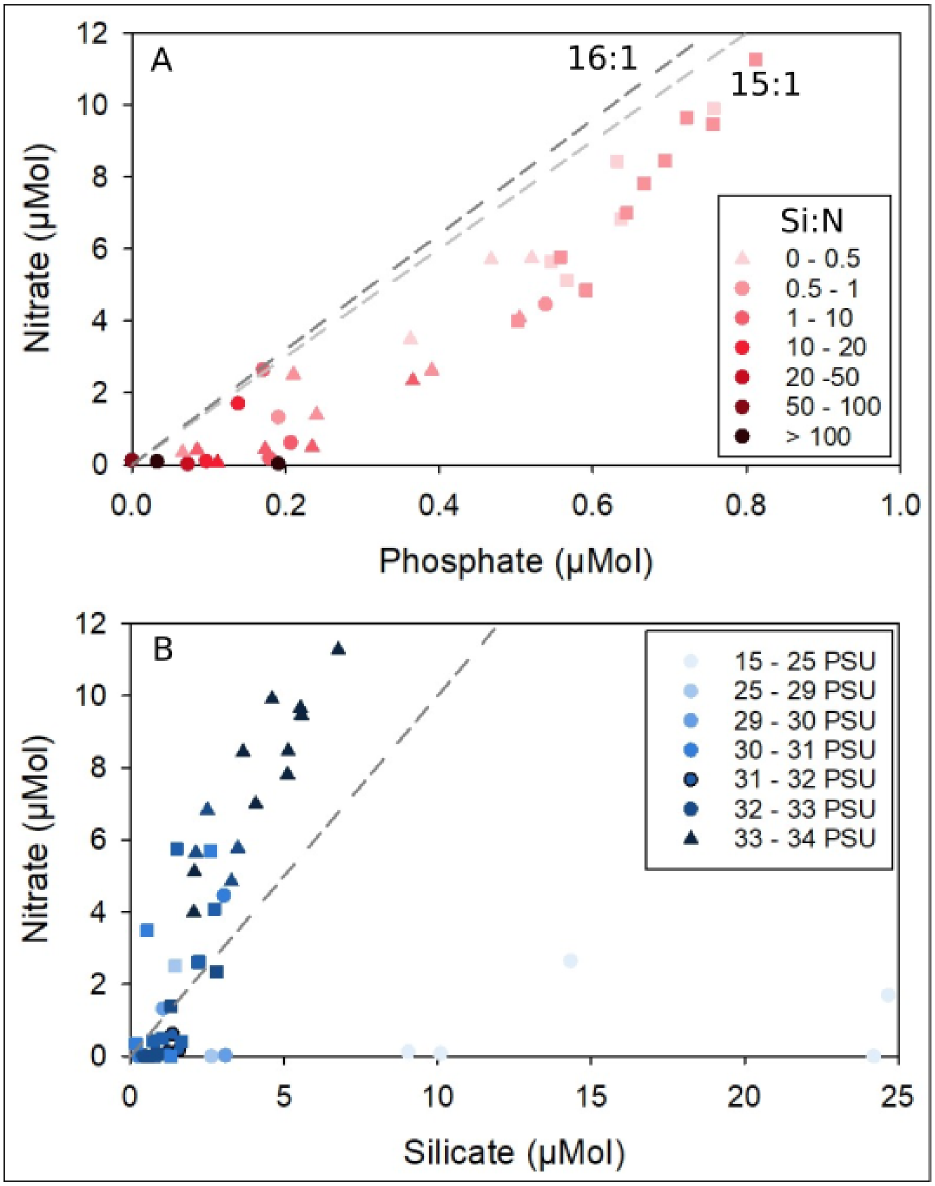

Figure S3. Scatter plots showing nutrient stoichmetry of Nuup Kangerlua and Ameralik Fjord. A) Nitrate versus phosphate molar concentrations, colour-coded by Si:N molar ratio. Dashed lines show the 15:1 and 16:1 Redfield ratios. B) Nitrate versus silicate molar concentrations, colour-coded by salinity, with the 1:1 relationship shown by the grey dashed line. Different symbol shapes represent sample depths; circles = surface, triangles = Chla-max, squares = deep.

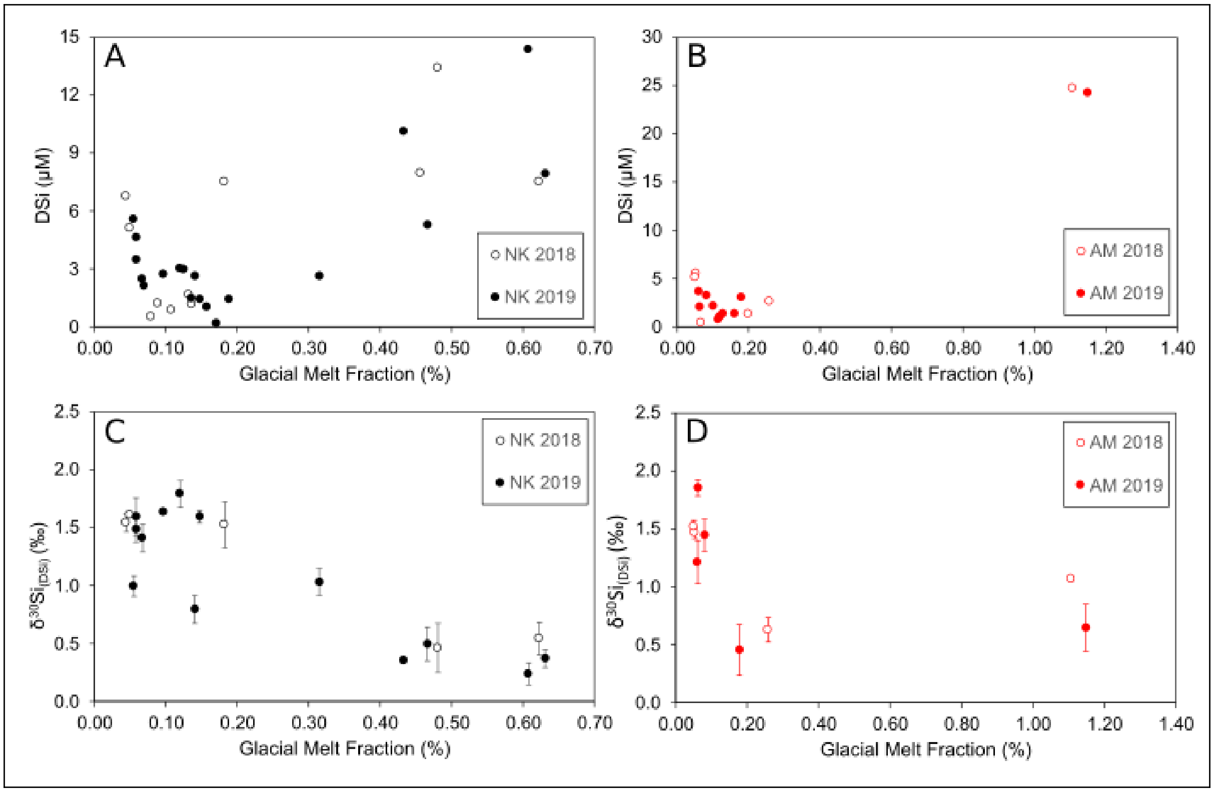

Figure S4. Scatter plots of dissolved silicon concentrations (DSi) and dissolved silicon isotopic composition ($\delta^{30}Si_{(DSi)}$) against glacial melt fraction (%). Open circles show data from July 2018 and closed circles show data from September 2019, with black symbols from Nuup Kangerlua and red symbols from Ameralik fjord. Errors represent 2 S.D calculated from triplicate sample measurements where possible. If less than triplicate measurements were analysed then an average sample and standard 2 S.D value of 0.12 ‰ was used.

Treatment	$\delta^{29}Si$ (‰)	$\delta^{30}Si$ (‰)	Difference from 0.51 gradient	Mg Correction
UV 24hrs + H_2O_2 at 1hr	0.31	1.69	-0.55	0.18
UV 24hrs + H_2O_2 at 1hr	1.04	2.22	-0.09	0.18
UV 24hrs + H_2O_2 at 1hr and 10hrs	0.88	1.72	0.01	0.31
UV 24hrs + H_2O_2 + O_2 bubbling	3.99	7.92	-0.04	-0.28 *
0.02µm filtered	0.25	0.45	0.02	0.24
0.02µm filtered	0.20	0.45	-0.03	0.24
0.02µm filtered	0.24	0.50	0.06	0.13

*Plus, large internal errors and very unstable signal. ^{28}Si intensity ranged from 2 to 40 volts within a 20-cycle period

Table S1. Summary of isotopic data during systematic testing of sample preparation methods for a particular sample (GF15-Surface).

Location	DSi (µM)	$\delta^{30}Si_{DSi}$ (‰)	Source
Leverett Glacier, SW Greenland. 2015 Season Average	20.8	- 0.25	Hatton et al., 2019a
Sub-Arctic Glacier Compilation Average	31.7	+ 0.16	Hatton et al., 2019b
Sub-Arctic Glacier Compilation Upper Quartile	31.7	+ 0.51	Hatton et al. 2019b
Langjökull Ice Cap, Iceland	49.4	- 0.58	Hatton et al. 2019b

Table S2. Glacial Endmembers used in Fractionation Model

Location	DSi (µM)	$\delta^{30}Si_{DSi}$ (‰)	Source
Average Fram Strait	8.8 ± 0.7	+ 1.79 ± 0.08	Brzezinski et al. 2021
Fram Strait Surface	11.1 ± 2.2	+ 1.92 ± 0.07	Brzezinski et al. 2021
Fram Strait CBDW + EBDW	11.9 ± 0.2	+ 1.64 ± 0.01	Brzezinski et al. 2021

Table S3. Seawater Endmembers used in Fractionation Model

Station	Year	Depth (m)	Salinity (PSU)	Nitrate (µM)	DSi (µM)	Phosphate (µM)	N : Si : P (µM)	Si:N (µM)
AM3	2018	5	32.4	0.02	0.42	0.07	0.3 : 5.8 : 1	22.9
AM3	2018	15	33.0	1.40	1.33	0.24	5.8 : 5.6 : 1	1.0
AM3	2018	400	33.4	8.46	5.14	0.69	12.2 : 7.4 : 1	0.6
AM7	2018	5	30.9	0.00	0.27	0.01	0 : 23.6 : 1	
AM7	2018	20	32.8	0.00	0.59	0.06	0 : 10.3 : 1	
AM7	2018	200	33.2	9.65	5.53	0.72	13.4 : 7.7 : 1	0.6
AM10	2018	0.5	24.0	0.12	9.05	-	-	73.9
AM12	2018	0.5	0.1	1.70	24.67	0.14	12.3 : 179 : 1	14.5
AM3	2019	3	31.0	0.62	1.37	0.21	3.0 : 6.6 : 1	2.2
AM3	2019	15	31.8	2.62	2.22	0.39	6.7 : 5.7 : 1	0.8
AM3	2019	100	32.5	4.85	3.29	0.59	8.2 : 5.6 : 1	0.7
AM7	2019	3	29.8	0.03	3.10	0.19	0.1 : 16.2 : 1	113.9
AM7	2019	10	31.4	0.44	0.74	0.17	2.5 : 4.2 : 1	1.7
AM7	2019	150	33.1	3.99	2.07	0.50	7.9 : 4.1 : 1	0.5
AM10	2019	3	30.7	0.00	1.34	0.09	0 : 14.4 : 1	-
AM10	2019	15	31.8	0.50	1.04	0.23	2.1 : 4.5 : 1	2.1
AM10	2019	200	33.1	8.44	3.67	0.63	13.4 : 5.8 : 1	0.4
AM12	2019	0.5	0.5	0.00	24.2	0.03	0.0 : 820 : 1	
GF3	2018	2	32.0	0.18	1.58	0.18	1.0 : 8.9 : 1	8.8
GF3	2018	5	31.7	0.10	1.23	0.10	1.1 : 12.8 : 1	11.9
GF3	2018	18	32.4	2.34	2.81	0.37	6.4 : 7.7 : 1	1.2
GF3	2018	15	33.3	7.81	5.12	0.67	11.7 : 7.7 : 1	0.7
GF7	2018	5	29.0	-	7.52	0.01	0 : 730 : 1	-
GF7	2018	18	32.1	0.07	0.86	0.11	0.6 : 7.7 : 1	12.6

GF7	2018	200	33.3	7.00	4.08	0.64	10.9 : 6.3 : 1	0.6
GF10	2018	10	31.1	0.42	1.67	0.08	4.9 : 19.7 : 1	4.0
GF10	2018	75	33.2	5.12	2.08	0.57	9.0 : 3.7 : 1	0.4
GF10	2018	450	33.6	11.3	6.77	0.81	13.9 : 8.3 : 1	0.6
GF11.5	2018	5	20.5	0.78	13.4	0.02	38.6 : 659 : 1	17.1
GF2	2019	1	29.8	1.32	1.06	0.19	6.9 : 5.6 : 1	0.8
GF3	2019	3	30.3	4.46	3.05	0.54	8.3 : 5.7 : 1	0.7
GF3	2019	15	31.6	4.08	2.73	0.50	8.1 : 5.4 : 1	0.7
GF3	2019	100	32.9	5.77	3.50	0.56	10.4 : 6.3 : 1	0.6
GF5	2019	3	27.1	-	1.43	0.04	0 : 36.1 : 1	-
GF5	2019	15	30.2	3.49	0.55	0.36	9.6 : 1.5 : 1	0.2
GF7	2019	10	28.5	2.51	1.46	0.21	11.9 : 6.9 : 1	0.6
GF7	2019	200	33.3	9.47	5.56	0.76	12.5 : 7.4 : 1	0.6
GF10	2019	3	20.5	0.08	10.1	0.03	2.5 : 307 : 1	121.1
GF10	2019	20	31.1	5.75	1.51	0.52	11.0 : 2.9 : 1	0.3
GF10	2019	200	33.2	9.91	4.61	0.76	13.1 : 6.1 : 1	0.5
GF11.5	2019	3	16.2	2.65	14.3	0.17	15.5 : 83.9 : 1	5.4
GF11.5	2019	20	31.3	5.67	2.99	0.50	11.4 : 6.0 : 1	0.5
GF13	2019	15	30.8	5.71	2.62	0.47	12.2 : 5.6 : 1	0.5
GF13	2019	100	32.8	6.83	2.51	0.64	10.7 : 3.9 : 1	0.4
GF15	2019	10	30.4	0.34	0.18	0.07	5.2 : 2.8 : 1	0.5
GF15	2019	100	32.8	5.65	2.13	0.55	10.3 : 3.9 : 1	0.4

Table S4. Nutrient Data for Nuup Kangerlua and Ameralik Fjord

Closed System Model (15 PSU)							
Year	**Station ID**	**ASi Dissolution Required (µM)**			**ASi as a proportion of average glacial ASi measured (%)**		
		ε = -0.74 ‰	**ε = -1.1 ‰**	**ε = -1.24 ‰**	**ε = -0.74 ‰**	**ε = -1.1 ‰**	**ε = -1.24 ‰**
2018	GF12	8.95	12.1	13.0	15.4	20.8	22.4
2018	GF10	0.47	1.98	2.44	0.81	3.41	4.20
2019	GF15	8.35	11.4	12.3	14.4	19.6	21.2
2019	GF13	12.9	16.7	17.87	22.3	28.8	30.8
2019	GF10	14.4	18.1	19.3	24.9	31.3	33.3
2019	GF7	2.58	3.99	4.42	4.45	6.88	7.62
2019	GF5	0.93	1.64	1.86	1.60	2.83	3.20
2019	GF3	0.74	1.73	2.03	1.27	2.99	3.51
Open System Model (15 PSU)							
Year	**Station ID**	**ASi Dissolution Required (µM)**			**ASi as a proportion of average glacial ASi measured (%)**		
		ε = -0.74 ‰	**ε = -1.1 ‰**	**ε = -1.24 ‰**	**ε = -0.74 ‰**	**ε = -1.1 ‰**	**ε = -1.24 ‰**
2018	GF12	6.49	8.39	8.98	11.2	14.5	15.5
2018	GF10	-	0.20	0.49	-	0.35	0.84
2019	GF15	5.44	7.05	7.54	9.38	12.2	13.0
2019	GF13	9.99	12.4	13.1	17.2	21.4	22.6
2019	GF10	12.1	14.7	15.5	20.8	25.3	26.7
2019	GF7	0.89	1.47	1.65	1.53	2.54	2.85
2019	GF5	-	0.22	0.29	-	0.37	0.50
2019	GF3	-	0.02	0.16	-	0.04	0.27

Table S5. ASi dissolution required for each surface sample in Nuup Kangerlua to correct modelled $\delta^{30}Si_{DSi}$ composition and observed $\delta^{30}Si_{DSi}$ values.